PHYSICAL REVIEW A VOLUME 8, NUMBER 3 SEPTEMBER 1973

Electron Decay-in-Flight Spectra from Autoionizing States of Highly Stripped Oxygen, Fluorine, Chlorine, and Argon Ions*

D. J. Pegg, I. A. Sellin, R. Peterson, and J. R. Mowat
University of Tennessee, Knoxville, Tennessee, 37916
Oak Ridge National Laboratory, Oak Ridge, Tennessee, 37830

W. W. Smith
University of Connecticut, Storrs, Connecticut 06268

M. D. Brown and J. R. MacDonald
Kansas State University, Manhattan, Kansas 66506
(Received 19 April 1973)

We report the results of spectroscopic studies of electrons associated with the decay in flight of metastable autoionizing states in three-, four-, five-, and eleven-electron heavy ions. The binding energies of a large number of observed states are found to be in good agreement with theoretical predictions (c.f. the companion paper of Junker and Bardsley) where such values are available. The lifetime of the lowest-lying quartet state, $(1s\,2s\,2p)\,^4P^o_{3/2}$ has been measured in three-electron oxygen, fluorine, chlorine, and argon ions. Competition between autoionizing and (in some cases forbidden) radiative-decay modes is discussed. There is evidence that the formation of metastable autoionizing states is quite a general phenomenon, occuring in a wide variety of atomic systems. A need for more extensive energy-level and lifetime calculations is readily apparent.

INTRODUCTION

The normal one-electron spectrum of an atomic system results from radiative transitions between discrete bound states which lie in energy below the first-ionization potential of the system. These states are formed from singly excited configurations in which the least tightly bound (valence) electron is transferred to higher shells. Some processes, however, can lead to the formation of states of much higher excitation, which lie above the first and often even higher ionization potentials. Core excitation refers to the raising of one or more electrons from an inner core to outer shells. Multiple-excitation processes involve (i) two or more electrons being simultaneously transferred from the valence shell to outer shells, or (ii) this same process accompanied by the excitation of one or more core electrons. Highly excited configurations resulting from these types of excitation processes will contain two or more "active" electrons (including electron-hole pairs) in different orbitals which couple together in the usual manner to form the state. Since few restrictions are imposed by the Pauli principle on this coupling, states of high total angular momentum and spin can result. For example, the spins of the active electrons can add to form a total spin equal to the algebraic sum of the individual spin angular momenta. Such states are often metastable against autoionization (because of the spin conservation rule on allowed autoionizing transitions) since the adjacent continuum states frequently have different multiplicity. States of high angular momentum can thus be metastable against both autoionization and electric dipole radiation simultaneously.

A spectroscopic study has been made of electrons emitted in flight by fast beams (~0.2–2 MeV/nucleon) of highly stripped heavy ions (O, F, Cl, Ar) following their passage through thin carbon-foil targets. The electrons arise from the decay of autoionizing states associated with the various ions present in the foil-excited beam. One of the principal features of the work described here is the observation of a large number of previously unknown autoionizing states, and while many of these states had not been previously predicted, the recent variational calculations of Junker and Bardsley[1] (see preceding paper) have aided us greatly in identification. In the text which follows we summarize the spectra and lifetimes discussed in our previously published work[2] together with more recent data.

Our interest in this work stems historically from the earlier observations[3] of the existence of a bound state associated with the three-electron helium ion, He^-. Wu[4] suggested that the $(1s2s2p)^4P^o_{5/2}$ state of He^- would be bound, and since it was expected to be also metastable against both autoionization and radiation, it accounted for the observations. Subsequent studies such as those by Wu and Shen,[5] Holøien and Midtal,[6] Garcia and Mack,[7] and Holøien and Geltman[8] were directed

at the study of those highly excited states which were metastable against autoionization. Later, Herzberg and Moore[9] suggested that lines that had been observed[10] in the lithium optical spectrum and which failed to fall into the normal classification scheme for singly excited configurations were in fact due to radiative transitions between doubly or core-excited states of lithium that were metastable against autoionization. More recently these types of transitions have been studied[11] optically in other three-electron ions using the foil-excitation method. Satellite lines on the long-wavelength side of the resonance lines of two-electron ions were first observed by Edlén and Tyrén[12] who interpreted them as arising from radiative transitions between doubly or core-excited states and the normal singly excited three-electron ion states. Similar optical lines have also more recently been observed in both laboratory plasma[13] and solar sources.[14]

Feldman and Novick[15] experimentally studied the forbidden autoionizing decay of metastable autoionizing states in several of the alkali atoms. The binding energy of the $(1s2s2p)\,^4P^o_{5/2}$ level in lithium was determined and its lifetime measured by observing the change in the charge states of an electron-impact excited lithium beam following autoionization in flight. Blau, Novick, and Weinflash[16] used a similar method to measure the lifetime of the corresponding state in He^-. The $(1s2s2p)\,^4P^o_{5/2}$-state lifetime was studied in other three-electron ions ($Z=4$–8) by Dmitriev *et al.*,[17] who also used a time-of-flight technique, to track the charge change in a fast foil-excited accelerator beam. Manson[18] and Balashov *et al.*[19] have calculated the lifetime of this lowest-lying quartet state in several ions of the lithium sequence. The present experimental method is similar to that used by Dmitriev *et al.* with the important exception that our method includes energy analysis of the emitted autoionization electrons which we believe represents a considerable advance over the previous time-of-flight methods.

THEORETICAL CONSIDERATIONS

The autoionization process arises from the coupling of a bound (or quasibound) state to a one-electron continuum state adjacent to it in energy. An electron is emitted in the transition with a kinetic energy equal to the difference in the electronic binding energies of the initial state and the final state of the residual ion. An allowed (Coulomb) autoionization process (which is induced by electrostatic interactions among the electrons) will occur if J, L, S, and parity are all conserved in the transition. When Coulomb autoionization is forbidden, autoionization may still occur via the relativistic magnetic interactions such as spin-orbit, spin-other-orbit, and spin-spin interactions. The lifetime of a state against autoionization is of course determined by the strength of the coupling to the continuum. States which make allowed autoionizing transitions are often very short lived ($\sim 10^{-12}$–10^{-16} sec) due to the strong coupling induced by the electrostatic interactions. Lifetimes against forbidden autoionizing transitions are of the order of α^4 times longer (in neutral atoms) than for lifetimes against allowed processes due to the weaker coupling to the continuum via the magnetic interactions. The strengths of the magnetic interactions increase with Z so that the autoionization lifetimes of these metastable states in highly stripped heavy ions can be fairly short ($\sim 10^{-8}$–10^{-10} sec) and thus effectively compete with radiative decay modes. Radiative transitions may occur between the metastable autoionizing states themselves or between one such state and nonautoionizing lower-lying bound states of the same system. In the case of three-electron ions, metastable quartet states can make allowed radiative transitions to lower-lying quartets but the lowest-lying quartet state will of course be

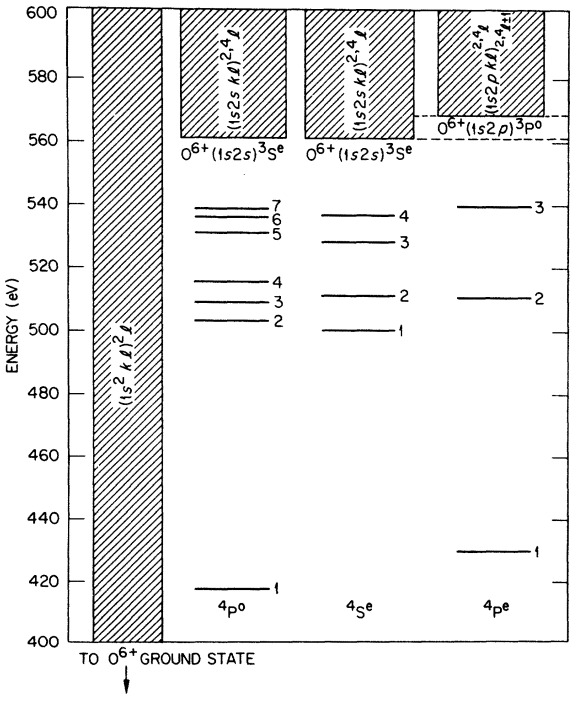

FIG. 1. Partial energy-level diagram showing some metastable quartet autoionizing states of three-electron oxygen. The energies indicated are from Ref. 1, measured with respect to the two-electron oxygen ground state.

metastable against electric dipole radiation as well as autoionization. Spin-forbidden radiative transitions to lower-lying doublets may also occur and the transition probabilities for these processes will increase with Z. Thus it has been observed,[20] for example, that forbidden radiative processes effectively compete with the forbidden autoionization for the decay of the lowest-lying quartet state, $(1s2s2p)\,^4P^o_{5/2}$, in highly stripped three-electron ions. In addition, there usually exists a differential metastability among the fine structure (J) levels within a particular state because of the different strengths of their coupling to the continuum states and because radiative transitions out of some of the levels are more probable than out of others.

Figure 1 shows the energies of some quartet states associated with the three-electron oxygen ion (O^{5+}). The energies shown in the figure are those predicted by Junker and Bardsley[1] and represent the excitation energies of the states above the ground state of the two-electron ion, which in this case is the final state of the residual helium-like ion after an autoionizing decay. It can be seen from the figure that different series of metastable levels arise as the quartet states converge on corresponding series limits, which are determined, in this case, by the first-excited triplet states of the two-electron oxygen ion. A quartet state lying in energy below this series limit will be adjacent to a doublet continuum state, making it metastable against autoionization. If the state lies above the series limits indicated, it will no longer be metastable, since it will then be adjacent to a quartet continuum. Thus, in general, the possible energies of electrons emitted in the decay of metastable autoionizing states will be determined by the corresponding range of energies in which the initial states are adjacent in energy to one-electron continuum states of different total spin. This range is quite large for residual two-electron ions, owing to the tight binding of the closed-core ground state, and so the autoionizing electrons that we observe from three-electron ions are of relatively high energy. A similar situation will arise for metastable autoionizing states of all alkalilike ions because of the tight binding, in general, of the final state of the residual inert-gas-like core.

EXPERIMENTAL METHOD

In these experiments we have used the ORNL tandem accelerator and/or the Oak Ridge Isochronous Cyclotron to produce fast ion beams of oxygen, fluorine, chlorine, and argon in the energy range 2–90 MeV. The beams were passed through thin carbon foils of nominal thicknesses ~ 5–30 $\mu g/cm^2$ which served to both strip and excite the ions of the beam. The emerging beam

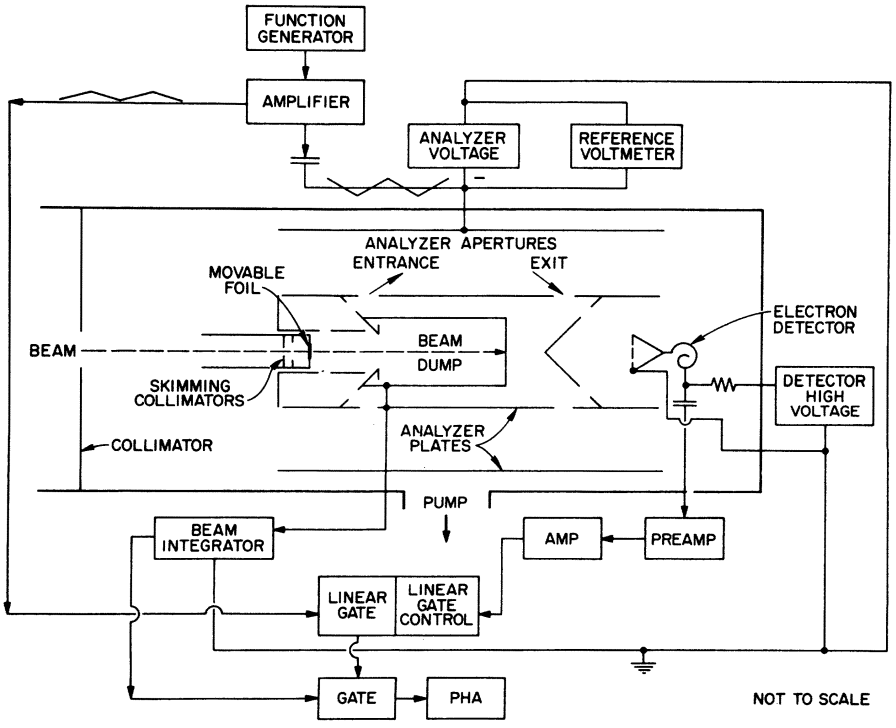

FIG. 2. Diagram of the apparatus. The cylindrical-mirror electrostatic electron-energy analyzer is shown schematically in a plane containing the beam axis.

contained a distribution of ionic-charge states whose spectrum is determined by the incident beam energy. In practice there are only three or four different ionic-charge states present in the beam with appreciable abundance. Beam energies were chosen for oxygen and fluorine to optimize the production of two-, three-, four-, and five-electron ions, for chlorine to optimize the production of three- and eleven-electron ions, and for argon three-electron ions only.

Figure 2 shows a schematic diagram of the apparatus used to obtain the spectra of the electrons emitted in flight by the foil-excited beam constituents following the decay of autoionizing states. Electrons emerging from the beams at polar angles near 42° were collected and energy-analyzed using a double-focusing cylindrical-mirror analyzer of the type described by Zashkvara *et al.*[21] The electrons were counted at the exit slit of the spectrometer with an electron multiplier, and these counts were normalized to fixed amounts of charge collected in the Faraday cup. The azimuthal slit symmetry about the beam direction provides high-electron collection efficiency compared to many other electron-spectrometer designs. The whole spectrometer was magnetically shielded against stray fields.

There were two modes of operation each characterized by different collimator and foil-target placements. In one arrangement a collimator system defined the beam before passage through the foil, as is shown in Fig. 2. Multiple scattering in the foil degrades the resolution somewhat in this arrangement especially for lower-energy heavy-ion beams, but this mode of operation is essential if one wishes to obtain data with the foil target very near or in the field of view of the spectrometer entrance slits. The advantage of such an arrangement is that short-lived autoionizing states can be observed to decay. Another operational mode which we have used to study the longer-lived metastable autoionizing states is one in which the foil target precedes the beam-defining collimators, a situation in which multiple scattering becomes less important. The spectra and lifetimes which we have published previously[2] were obtained using this latter arrangement. In both modes of operation the position of the foil with respect to the spectrometer viewing region is adjustable, thus facilitating time-of-flight lifetime measurements. By using ion beams with velocities of ~ 10^9 cm/sec (~ 1 MeV/amu) it has been possible to track, over a range up to 80 cm, the decay of many metastable autoionizing states. Electron spectroscopy is also greatly facilitated by the ability to move the foil target, since the differential metastability of the various emitting ions produces dramatic changes in the spectrum shape as a function of target position. Blended peaks are frequently *spatially* resolved in this manner.

Figure 3 shows a spectrometer transmission curve obtained with electrons elastically scattered from a neon-gas target. The intrinsic resolution is under some circumstances degraded somewhat in the actual beam experiments by kinematic broadening arising from the high velocity of the emitting ions, their energy straggling, and a finite acceptance angular spread (about 1° in our present geometry). Misalignment of the spectrometer axis with respect to the beam axis of a fraction of a degree can cause kinematic energy shifts and distortion of the observed spectral features. For our present geometry, kinematic spreads of a few eV out of 1 keV are quite common. The kinematic transformation relationships are derivable from two equations which relate (nonrelativistically) the laboratory electron velocity v_L and emission angle θ_L to the beam velocity v_B and the ionic-rest-frame emission velocity v_0 and angle θ_0:

$$v_L \cos\theta_L = v_B + v_0 \cos\theta_0 , \tag{1}$$

$$v_0^2 = v_L^2 + v_B^2 - 2 v_B v_L \cos\theta_L . \tag{2}$$

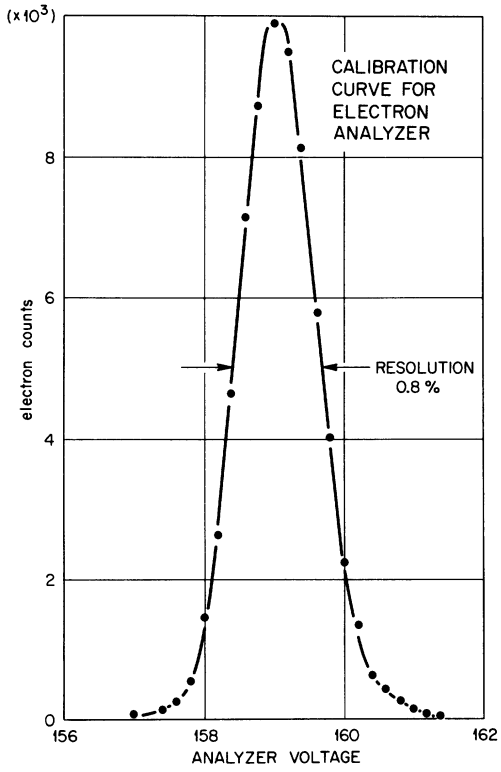

FIG.3. Electron-spectrometer transmission curve, obtained with electrons elastically scattered from a neon-gas target.

Another familiar phenomenon which occurs is the kinematic peaking in the forward direction of the angular distribution of the emitted electrons in the laboratory system. A particularly simple and useful form of the ratio of the solid angle in the ionic rest frame ($d\Omega_0$) to that in the laboratory frame ($d\Omega_L$) can be easily derived by implicit differentiation of Eqs. (1) and (2). The result is

$$\frac{d\Omega_0}{d\Omega_L} = \frac{(v_L/v_0)^2}{(v_L/v_0) - (v_B/v_0)\cos\theta_L} . \tag{3}$$

The condition that the denominator of Eq. (3) dis-

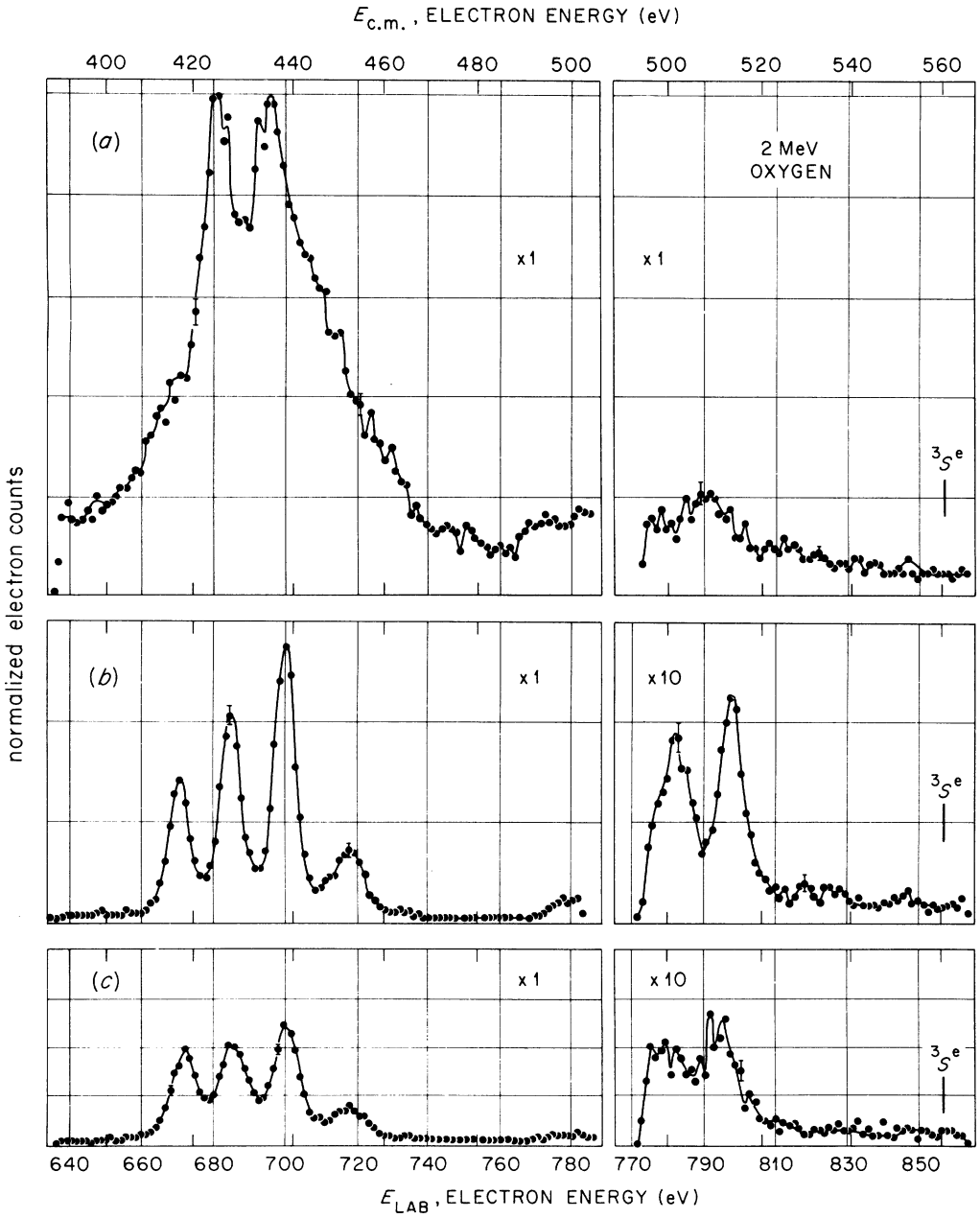

FIG. 4. Spectra of autoionization electrons emitted by 2-MeV oxygen ions undergoing decay in flight, plotted in both the laboratory frame and rest frame of the emitting ion. The energy scale is divided, separating the "low" and "high" energy group of peaks. The expansion factors shown normalize the intensity scales to that of the spectrum in the top left-hand corner. Spectrum (*a*) refers to "foil-zero" position; (*b*) and (*c*) refer to time delays of 0.7 and 1.0 nsec, respectively, with respect to (*a*). The smooth curve drawn through the data is to guide the eye.

appear corresponds to the existence of a maximum emission angle for the electrons in the laboratory frame given by

$$\sin\theta_L(\max) = v_0/v_B \quad \text{for } v_B > v_0 . \tag{4}$$

Near this maximum angle, a large range of laboratory electron energies is emitted into the range of angles accepted by the electron spectrometer (for a given ionic-rest-frame energy). The spectrometer resolution then degenerates very badly from its normal value because of this kinematic effect, and no useful spectra can be obtained at $\theta = \theta_L(\max)$.

RESULTS

Spectra

Figures 4–7 show spectra of autoionization electrons emitted in flight by fast oxygen- and fluorine-ion beams following passage through carbon foils of nominal thicknesses ~ 5–30 $\mu g/cm^2$. The positions of prominent features observed in these spectra as well as from other data not shown here are tabulated in Table I, together with theoretical predictions of the energies of some multiply and core-excited metastable autoionizing states of three-, four-, and five-electron

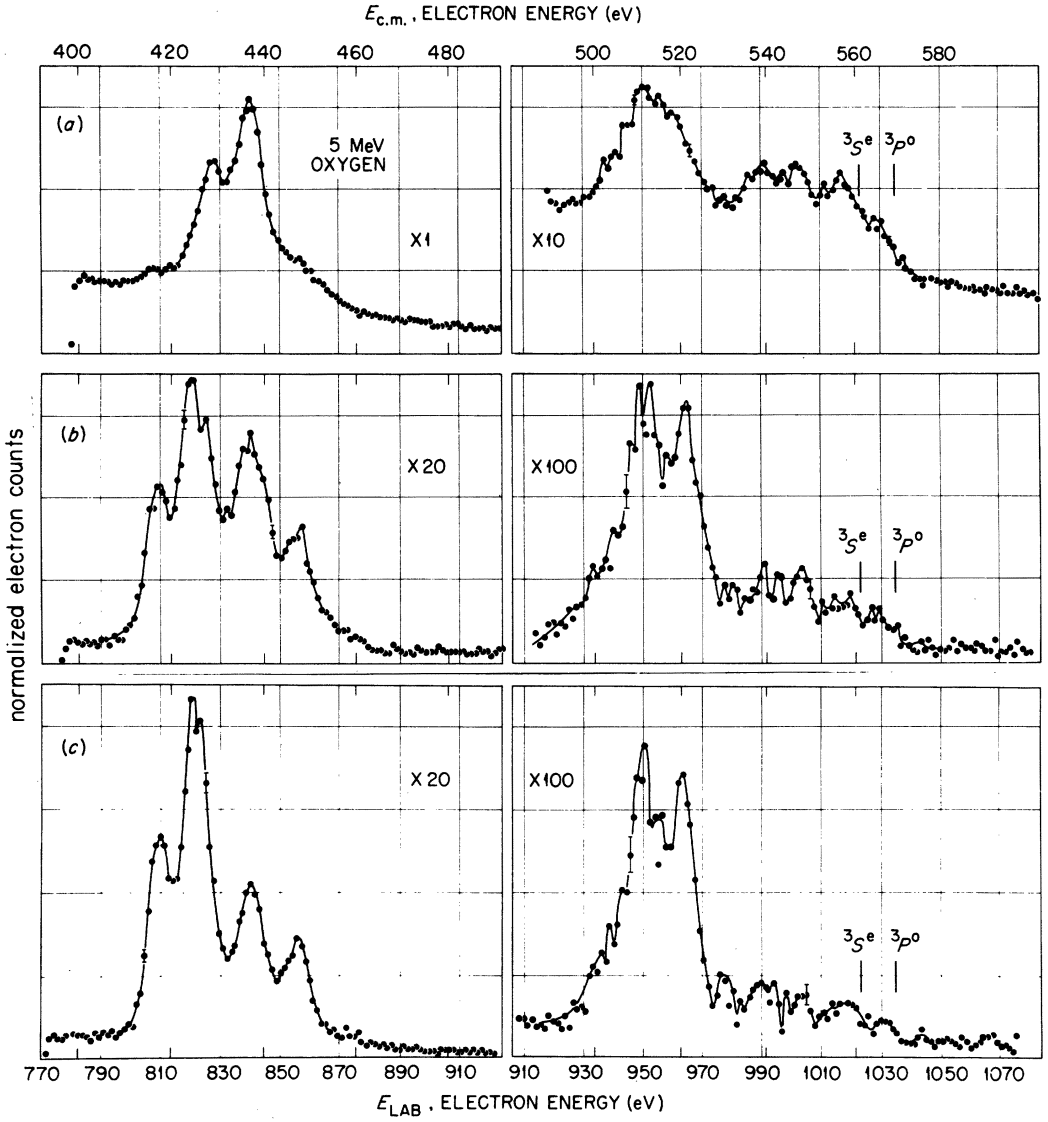

FIG. 5. Spectra of autoionization electrons emitted by 5-MeV oxygen ions undergoing decay in flight. Spectra (*b*) and (*c*) refer to time delays of 0.3 and 0.7 nsec, respectively, with respect to (*a*). For other information, see caption to Fig. 4.

oxygen and fluorine ions. The energies shown in the table are the emission energies of the autoionization electrons in the ionic rest frame. The absolute energies of the spectral lines are subject to certain systematic errors. The chief contributions to these errors stem from uncertainties in the foil thickness (the effective foil thickness can increase during the course of an experiment) and from small variations in the angle of admittance to electron spectrometer with steering of the ion beam. Foil-thickness uncertainty implies an uncertainty in energy loss of the ions in the foil and

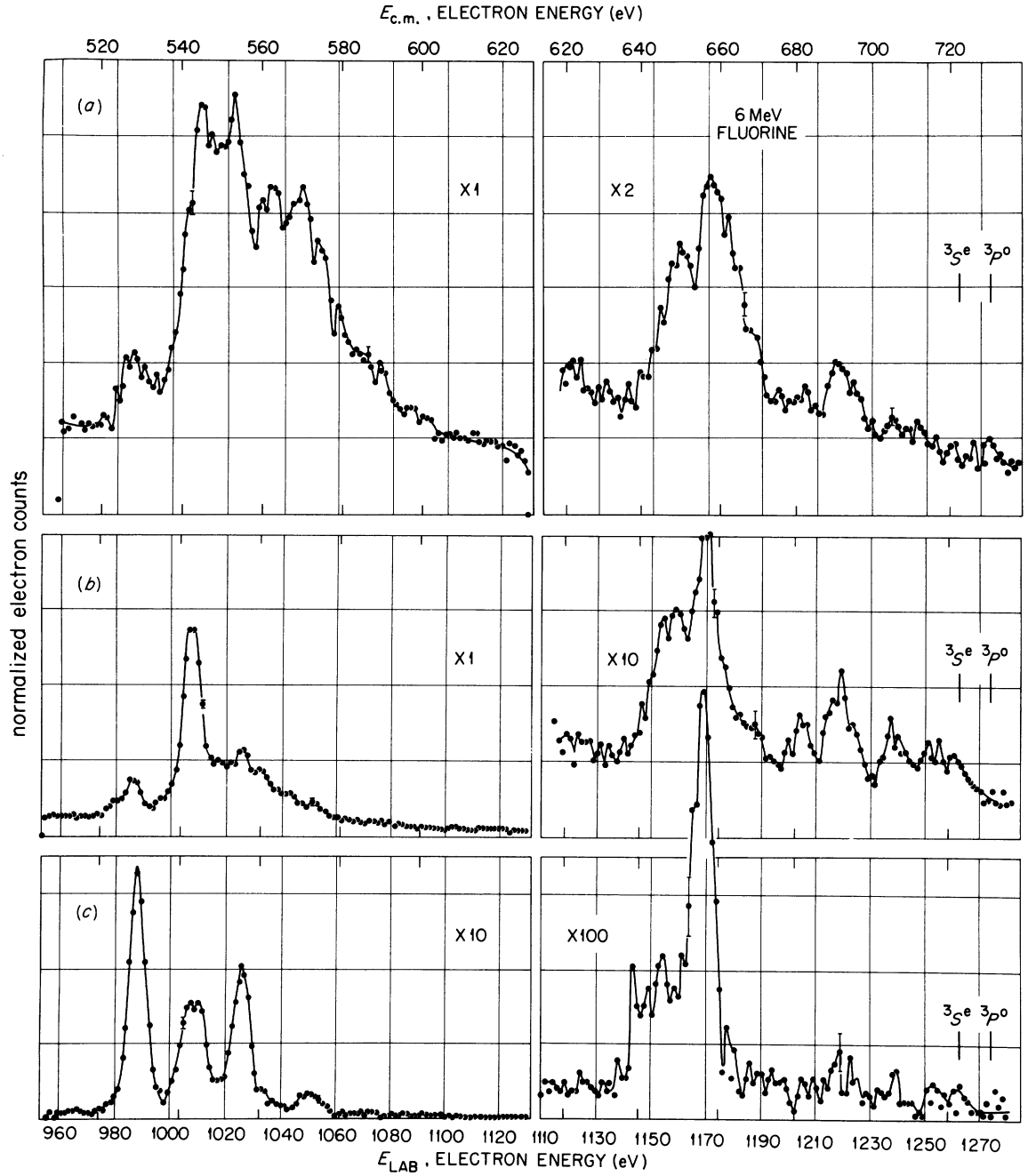

FIG. 6. Spectra of autoionization electrons emitted by 6-MeV fluorine ions undergoing decay in flight. Spectra (*b*) and (*c*) refer to time delays of 0.1 and 0.4 nsec, respectively, with respect to (*a*). For other information, see caption to Fig. 4.

hence in both the energy and energy spread of the emergent beam. These systematic uncertainties contribute to kinematic peak shifts when the laboratory energies are transformed to those of the emitting ions' rest frame. We estimate an uncertainty of ± 3 eV to the absolute energies of the individual peaks, although the energies of the more prominent and resolved features *relative* to the lowest-lying peak in each spectrum are better known (~ ± 1 eV). Table I indicates that the energies of many of the features we observe are in good agreement with the calculated energies of metastable autoionizing states of three-electron oxygen and fluorine ions arising from such highly excited configurations as

$1s2sns\,(n\geq 3)$, $1s2snp\,(n\geq 2)$, $1s2snd\,(n\geq 3)$,
$1s2snf\,(n\geq 4)$, $1s2pnp\,(n\geq 2)$, $1s2pnd\,(n\geq 3)$,
etc.

The theoretical predictions for three-electron ions have been made, in an accompanying paper, by Junker and Bardsley,[1] and earlier, to a lesser extent, by Holøien and Geltman.[8] Variational techniques were used by both these investigators, although slightly different trial wave functions were used in each case. Berry[22] has made simple semiempirical estimates of the energies of quartet states with configurations such as $1s2snl\,(n\geq 3)$ and $1s2pnl\,(n\geq 3)$ in three-electron ions by using the quantum-defect method, with zero quantum defects, a situation approximately applicable to nonpenetrating orbits such as those for $l\geq 2$. The notation used in Table I and elsewhere in this paper is that used previously by Holøien and Geltman.[8] Rigorously speaking, none of these states will originate from a single pure configuration, owing to mixing with neighboring configurations of the same symmetry. However, in many cases certain single configurations will dominate, especially for lower-lying terms. We have indicated in Table I the dominant configurations for certain cases to aid understanding of the notations and to exhibit the high principal quantum numbers and excitation energies involved. For example, the $^4P^o(1)$ state in oxygen, whose configuration is $1s2s2p$, involves an excitation energy (with respect to the three-electron oxygen ground state) of approximately 555 eV. Table I also shows the theoretical predictions of Junker and Bardsley[1] for the energies of some metastable autoionizing states associated with four- and five-electron oxygen and fluorine ions. Recent variational calculations by Holøien and Midtal[23] predict the energies of some doubly excited states of two-electron ions ($2pnp$ configurations with $n=2$–6) that are metastable against autoionization. These calculations indicate that only the $^3P^e(1)$ state would fall within the energy range observed in the present experiment. This state, which is

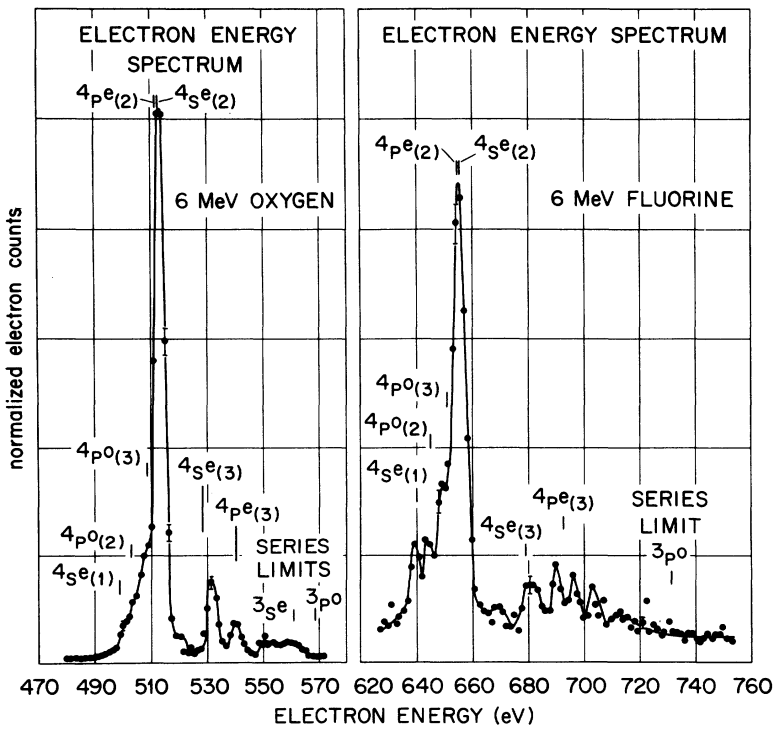

FIG. 7. Spectra of "high" energy group of electrons emitted by 6-MeV oxygen and fluorine beams undergoing decay in flight, plotted in ionic rest frame. Theoretically predicted values (Ref. 8) are shown for some metastable autoionizing states by a tick mark above the spectral features. The spectra were accumulated for time delays of 2–3 nsec after excitation.

TABLE I. Electron energies (eV, ionic rest frame) for some forbidden autoionizing transitions in three-, four-, and five-electron oxygen and fluorine ions. Theoretical predictions are due to Ref. 1 unless otherwise indicated. Dominant initial-state configurations are shown for certain representative states. Final states are the lowest-lying states of this symmetry, i.e., $(1s^2)\,{}^1S^e$, $(1s2p)\,{}^2P^o$, etc. The results of Ref. 8 have been adjusted to account for relativistic effects in a manner described in Ref. 1.

			Oxygen		Fluorine	
No. of electrons	Initial state	Final state	Theory	Expt. obsv.	Theory	Expt. obsv.
3	$(1s2s2p)\,{}^4P^o(1)$	${}^1S^e$	417.3, 416.2 [a]	417	531.3, 530.0 [a]	530
4	$(1s2s2p^2)\,{}^5P^e(1)$	${}^2P^o$	428.3	425, 427,	543.6	543, 545
3	$(1s2p^2)\,{}^4P^e(1)$	${}^1S^e$	429.5, 429.3 [a]	429	545.3, 545.1	
3	$(1s2p^2)\,{}^2P^e(1)$	${}^1S^e$	436.6		553.7	552
5	${}^6S^o(1)$	${}^3P^e$	438.8	436, 439	556.7	556, 557
4	${}^5P^e(1)$	${}^2S^e$	440.3	440	557.6	
4	${}^5S^o(1)$	${}^2P^o$	444.9	445, 449	562.9	562, 564, 567
4	$(1s2p^3)\,{}^3S^o(1)$	${}^2P^o$	453.7	453, 456	573.5	572, 574
5	${}^6S^o(1)$	${}^3P^o$	455.1		575.9	
4	$(1s2p^3)\,{}^5S^o(1)$	${}^2S^e$	456.9		576.9	578
4	${}^3S^o(1)$	${}^2S^e$	465.7		587.5	586, 589
4	${}^5P^o(1)$	${}^2P^o$	497.2		637.3	637
3	${}^4S^e(1)$	${}^1S^e$	500.2, 498.0 [a]	498, 500,	641.4, 638.6 [a]	
4	${}^5S^e(1)$	${}^2P^o$	500.5	503	641.8	640, 643
4	${}^5P^e(2)$	${}^2P^o$	501.4		643.0	
5	${}^6S^o(2)$	${}^3P^e$	502.2			
3	${}^4P^o(2)$	${}^1S^e$	503.9, 502.3 [a]		645.8, 643.6 [a]	
4	${}^5P^o(2)$	${}^2P^o$	505.1	505, 507	647.4	645
3	${}^4D^e(1)$	${}^1S^e$	505.8, 506.3 [b]		647.8, 649.9 [b]	
3	${}^4P^o(3)$	${}^1S^e$	508.2, 508.0		650.3, 650.1 [a]	
4	${}^5P^o(1)$	${}^2S^e$	509.2		651.1	
4	${}^5P^e(3)$	${}^2P^o$	509.5		651.8	
3	$(1s2s4d)\,{}^4D^e(2)$	${}^1S^e$	510.0		652.4	
3	${}^2P^e(2)$	${}^1S^e$	510.2		652.7	
3	${}^4S^e(2)$	${}^1S^e$	511.1, 510.7 [a]		653.7, 654.2 [a]	
3	${}^4P^e(2)$	${}^1S^e$	511.5, 511.3 [a]		654.2, 654.1 [a]	
3	$(1s2s4f)\,{}^4F^o(1)$	${}^1S^e$	511.8		654.7	649, 651
4	${}^3S^o(2)$	${}^2P^o$	511.9	511, 513	654.9	654, 665, 659
3	${}^2D^o(1)$	${}^1S^e$	512.3		655.0	
4	${}^5P^o(3)$	${}^2P^o$	512.5		655.4	
4	${}^5S^e(1)$	${}^2S^e$	512.5		655.8	
4	${}^5P^e(2)$	${}^2S^e$	513.4		657.0	
3	${}^4D^o(1)$	${}^1S^e$	513.5, 513.9 [b]		656.4, 658.4 [b]	
4	${}^5S^o(2)$	${}^2P^o$	514.1		657.3	
3	${}^4P^o(4)$	${}^1S^e$	514.5		657.6	
5	${}^6S^o(2)$	${}^3P^o$	515.5		...	
5	${}^6S^o(3)$	${}^3P^e$	515.9		...	
3	${}^2P^e(3)$	${}^1S^e$	516.8	515, 517	660.3	
4	${}^5P^e(4)$	${}^2P^o$	517.1		661.0	661, 662
4	${}^5P^o(2)$	${}^2S^e$	517.1		661.4	
3	${}^2D^o(2)$	${}^1S^e$	518.4		662.2	
4	${}^5S^e(2)$	${}^2P^o$	520.8		670.3	670
4	${}^5P^e(3)$	${}^2S^e$	521.5	521	665.8	
4	${}^3S^o(3)$	${}^2P^o$	521.7		666.3	665
4	${}^3S^o(2)$	${}^2S^e$	523.9		668.9	
4	${}^5P^o(3)$	${}^2S^e$	524.5	524, 526	669.4	668, 670
4	${}^5S^o(2)$	${}^2S^e$	526.1		671.3	
4	${}^5P^e(4)$	${}^2S^e$	529.1		675.0	674
5	${}^6S^o(3)$	${}^3P^o$	529.2		...	
3	${}^4S^e(3)$	${}^1S^e$	529.9, 527.6		680.7, 677.9 [a]	
3	${}^4P^o(5)$	${}^1S^e$	530.8		681.7	
3	$(1s2s5d)\,{}^4D^o(3)$	${}^1S^e$	531.8	530, 532	682.9	
3	${}^4F^o(2)$	${}^1S^e$	532.6		683.8	681, 683
4	${}^5S^e(2)$	${}^2S^e$	532.8		684.3	685
4	${}^3S^o(2)$	${}^2S^e$	533.7		680.3	

TABLE I *(Continued)*

No. of electrons	Initial state	Final state	Oxygen Theory	Oxygen Expt. obsv.	Fluorine Theory	Fluorine Expt. obsv.
3	$(1s2s7p)\,^4P^o(6)$	$^1S^e$	535.9		687.3	
3	$^4D^e(4)$	$^1S^e$	536.4		687.9	
3	$^2P^e(4)$	$^1S^e$	536.8		688.4	
3	$^4S^e(4)$	$^1S^e$	536.9		688.4	
3	$^4P^e(3)$	$^1S^e$	537.1, 539.6 [a]	536, 539	688.6, 691.7	687, 690
3	$^4F^o(3)$	$^1S^e$	537.3		688.8	691
3	$^2D^o(3)$	$^1S^e$	537.4		688.9	
3	$^4D^o(2)$	$^1S^e$	537.8, 537.7 [b]		689.4, 690.7 [b]	
3	$^4P^o(7)$	$^1S^e$	538.1		689.7	
3	$^2P^e(5)$	$^1S^e$	542.3		694.7	
3	$^4S^e(5)$	$^1S^e$	542.5		697.7	695
3	$(1s2s9p)\,^4P^o(8)$	$^1S^e$	542.8	542, 545	697.9	698
3	$^2D^o(4)$	$^1S^e$	543.0		695.5	
3	$^4F^o(4)$	$^1S^e$	543.6		698.9	695
3	$^4S^e(6)$	$^1S^e$	548.7		704.1	698
3	$^2P^e(6)$	$^1S^e$	548.7		704.3	
3	$^4P^e(4)$	$^1S^e$	548.7	548	704.3	
3	$^2D^o(5)$	$^1S^e$	548.7		704.3	702, 706
3	$(1s2s8f)\,^4F^o(5)$	$^1S^e$	548.7		704.4	
3	$^4D^o(3)$	$^1S^e$	549.0	552, 555	704.7	
				558, 566		709, 714
				569		717, 722
						731

estimated to occur at 470.67 and 591.20 eV in the two-electron oxygen and fluorine spectra, respectively, does not appear to be present in our spectra with detectable intensity, presumably because of the large branching ratio for radiative depopulation of the state by transitions to lower-lying singly excited triplets of opposite parity.

A feature that is common to all the spectra is the concentration of the electron peaks (from three-electron ions at least) into two basic groups, one of which is shown on the left in Figs. 4–6; the other group, of higher energy, appears toward the right of these figures. This higher-energy group is also shown separately in Fig. 7 for both oxygen and fluorine. The expansion factor indicated in each spectrum of Figs. 4–6 normalizes the intensity scale to that of the spectrum shown in the top left-hand corner of each figure. It is clear that the higher-energy group of states is roughly an order of magnitude less intense than the peaks of the corresponding lower-energy group. For three-electron ions the lower-energy group arises from the lowest-lying quartets and doublets with configurations such as $1s2s2p$ and $1s2p^2$, in which the active electron or electrons are in the $n=2$ shell. Three-electron ion states in the higher-energy group of peaks arise from configurations which contain at least one electron in the $n=3$ shell or higher.

The labels (*a*), (*b*), and (*c*) attached to the spectra in Figs. 4–6 indicate that the data were accumulated at different distances from the foil, which is equivalent of course to corresponding time delays following excitation. One is thus able to observe the temporal decay of the features in going from foil positions (*a*) to (*b*) to (*c*). The foil-zero position itself is not very well defined in this type of experiment, since the finite-entrance-slit system of the electron spectrometer subtends a finite segment (a window) of the excited beam instead of an infinitesimal segment. This window is effectively about 0.0035 in. long with the present slit system and geometry. As a function of distance from the external downstream target position, a maximum in the count rate will not be recorded until the spectrometer viewing window is completely filled by the excited beam. This situation is approximately equivalent to the positions (*a*) in the spectra of Figs. 4–6, and so this position has been arbitrarily defined as the "foil-zero" position. The foil positions (*b*) and (*c*) then refer to certain time delays with respect to position (*a*). The actual delays are indicated in the captions accompanying the figures. It seems appropriate here to comment on the effect of the spectrometer viewing window on the observed intensities of the various spectral features. The exponentially decaying intensity of a

particular spectral line will also be accompanied by a further apparent attenuation due to the finite spectrometer viewing window. The product of the beam velocity and the state lifetime as compared to the length of beam defined by the spectrometer entrance slits determines the fraction of all the decays which will be observed. Specifically, the faster the rate of decay within the window, the greater the number of electrons that will be counted at any given foil position. This means that a long-lived state may produce a line which appears less intense in the spectrum than a shorter-lived state, which decays more rapidly within the viewing window. In the absence of quantitative lifetime estimates for a particular state, interpretations of the observed spectral-peak heights for that state are thus problematic.

It can be seen from Figs. 4–6 that the "foil-zero" spectrum (*a*) contains many unresolved short-lived features that decay away in the time delay between foil positions (*a*), (*b*), and (*c*). These features may be associated with Coulomb autoionizing states or metastable autoionizing states with strong radiative depopulation channels that tend to shorten the lifetime of the state. It is apparent that the spectroscopic analysis is greatly improved by allowing these short-lived states to decay away, leaving only the longer-lived peaks, as is shown in the spectra corresponding to foil positions (*b*) and (*c*). Even in these cases, it appears that many of the peaks are in fact blends of two or more closely lying features, this being particularly evident in the high-energy group of states, where it is difficult to draw an unambiguous smooth curve through the data. However, it is believed that most of the features observed and recorded in Table I are real, since they consistently appear in all our spectra, including unpublished data, at the same energies; and the peak intensities, although small, are definitely above the very low background of this energy region. It seems worthwhile to point out that there also consistently appears a drop in intensity coincident with the energies of the predicted series limits for metastable quartet and doublet states in three-electron ions. The evidence indicates (see Table I) that we are clearly observing the decay of metastable autoionizing states in three-electron oxygen and fluorine ions and in fact it appears that we observe very highly-excited quartet states close to the three-electron series limits with the principal quantum numbers of the outermost electrons at least $n = 8$ and orbital angular momenta up to at least $l = 3$. The combination of such high spin and orbital angular momenta will lead to high J levels. There will exist a differential metastability among the J levels of a particular term, and the level of highest total angular momentum will be the most metastable. For this reason it is probable that it is this component alone which is observed in the spectra taken at relatively large time delays after excitation.

TABLE II. Total binding energies (eV) of the $^4P^o(1)$ and $^4P^e(1)$ states in some three-electron ions.

State \ Z	8	9	17	18
$^4P^o(1)$ Expt.	−1193.7 (3.0)	−1526.5 (3.0)	−5655 (24)	−6369 (33)
	−1193.7 [a]	−1525.7 [a]	−5652 [b]	6352 [b]
Theory	−1193.1 [c]	−1525.7 [c]		
$^4P^e(1)$ Expt.	−1181.4 (3.0)	−1511.4 (3.0)	−5624 (24)	···
	−1180.7 [a]	−1510.8 [a]	···	
Theory	−1180.9 [c]	−1512.0 [c]		

[a] Reference 8.
[b] Extrapolated value from Ref. 8.
[c] Reference 1.

The spectral features associated with the lower-energy group of states are more intense and better resolved in some cases, especially in the spectra associated with foil positions (*b*) and (*c*). The observed energies of the lowest-lying peak in both the oxygen and fluorine spectra agree well with the theoretically predicted energies (see Table I) of the $^4P^o(1)$ state of three-electron oxygen and fluorine ions. The second peak in the spectra is observed to be due to the blend of at least two components which are sufficiently resolved in some cases to indicate that they may be due to the decay of a quintet state of four-electron ions and a quartet state of three-electron ions. Table I predicts that the third peak, which we have previously[24] called peak A, should also be a blend of three states from different charge-state ions and indeed several features appear within the energy range encompassed by peak A. A similar situation is true for the fourth prominent peak of the spectrum, which we have previously[24] called peak B. The possibility of the existence of states associated with four-electron ions being responsible for peaks A and B was previously[24] noted by us. Lowering the beam energy had enhanced both the relative size of peaks A and B as well as the four-electron beam fraction.

The total binding energies of the $^4P^o(1)$ states associated with three-electron oxygen, fluorine, chlorine, and argon ions are shown in Table II. The corresponding energies of the $^4P^e(1)$ states are also shown in the table for three-electron oxygen, fluorine, and chlorine ions. The total binding energies of these states are obtained by subtracting the autoionizing electron-emission energies, as measured in the ionic rest frame, from the sum of the well-established one- and two-electron ionization potentials.[25] The uncertain-

ties in the absolute binding energies of the states are quoted in parentheses after each experimental result. The theoretically predicted energies of these states in oxygen and fluorine are due to Holøien and Geltman[8] and Junker and Bardsley.[1] The estimates quoted for the three-electron chlorine and argon ions have been derived by extrapolating the nonrelativistic results of Holøien and Geltman[8] ($Z=2-10$) to the cases of $Z=17$ and 18. The extrapolation procedure involved a least-squares power-series expansion in decreasing powers of Z (beginning with Z^2). In the nonrelativistic limit this scaling is in principal exact, although errors of course will arise in the fitting procedure. We believe the fits are good, however, to ~ 1–2 eV. It should be pointed out that we have changed slightly (by 2 eV) the value previously quoted[26] as our best estimate of the binding energy of the $^4P^o(1)$ state in three-electron chlorine. Small corrections have also been made to our previously quoted[26] extrapolations of the theoretical values of Holøien and Geltman,[8] and all the corrected values are now shown in Table II. Snyder[27] has estimated relativistic corrections of -17.6 and -24.7 eV to the nonrelativistic energies of the $^4P^o(1)$ state in three-electron chlorine and argon, respectively. These corrections come mainly from the mass-velocity correction ($\sim -\frac{5}{4}\alpha^2Z^4$) to the single K-shell electron velocity and the Darwin correction ($\sim +1\alpha^2Z^4$). Table III shows that there exists good agreement between our experimental results and theory. The precision of the present experiment is comparable to each of the relativistic corrections terms, and were it not for their extensive cancellation, their separate effects might have been observed.

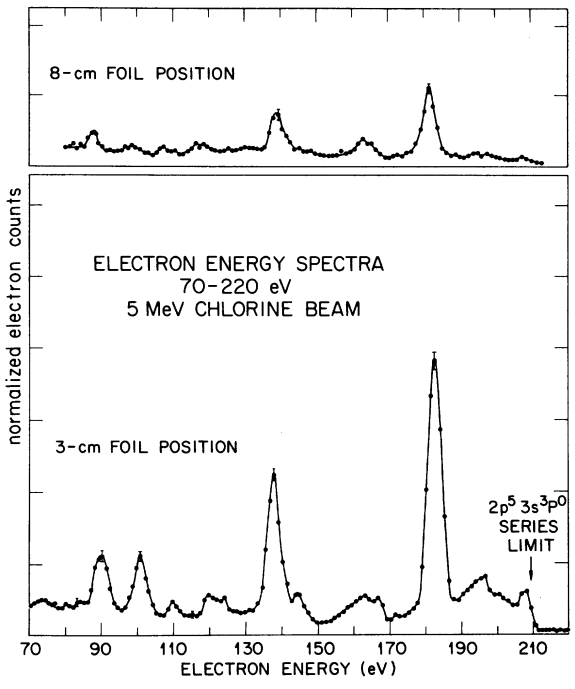

FIG. 8. Segment of autoionization electron spectra emitted by 5-MeV chlorine ions undergoing decay in flight, plotted in the ionic rest frame. Data are shown for two different target positions, 3 and 8 cm from the spectrometer viewing region.

It was noted earlier, by Feldman and Novick,[15] that there exist metastable autoionizing states associated with most of the alkalis, and we have searched for these states in sodiumlike chlorine (Cl^{6+}). The chlorine beam energy (~ 5 MeV) in this case was chosen to maximize the production of the eleven-electron charge-state component. At this energy ~ 30% of the emerging foil-excited beam is in this charge state, along with comparable fractions of both ten- and twelve-electron ions. Figure 8 shows spectra of autoionization electrons emitted from the foil-excited beam at two different distances (3 and 8 cm) downstream from the foil target. The electron energies are given in the rest frame of the emitting ion. The over-all spectral resolution is somewhat degraded in this experiment, probably because of the worsening of the multiple-scattering problem for low-energy heavy-ion beams. This energy-straggling effect could clearly become a serious limitation to the method for heavy ions at much lower beam energies. Firm identification of any of the spectral features shown in Fig. 8 is at present precluded by an almost complete lack of theoretical estimates of the energies and lifetimes of metastable autoionizing states, either in eleven-electron systems, or in any other adjacent charge-state systems that might be present in the beam. There is clearly now a need for such calculations. We believe, however, that many of the states observed in decay are quartet and possibly doublet states of eleven-electron chlorine that are metastable against autoionization, and the situation is somewhat analogous to that of the three-electron

TABLE III. Lifetimes (nsec) of the $(1s2s2p)\,^4P^o_{5/2}$ level in some three-electron ions.

Z	Present expt.	Other expts.	Theory
8	25 ± 3	40 ± 20 [a]	31,[b] 75 [c]
9	15 ± 1	···	···
17	0.91 ± 0.04	···	···
18	0.66 ± 0.04	···	···

[a] Reference 17.
[b] Reference 18.
[c] Reference 19.

systems. These states may be formed from such core-excited configurations as $2p^5(nl)(n'l')$ with $n, n' \geq 3$. It is conceivable that states of even higher total spin may arise from simultaneous excitation of two or more inner-shell electrons. The well-defined falloff in intensity at the high-energy end of the spectra is in good agreement with the series limit that would be expected for metastable quartet and doublet states associated with eleven-electron chlorine, i.e., the excitation energy of the lowest-lying triplet states of the ten-electron ion. The possibility that some of the spectral features arise from other adjacent charge-state ions also present in the beam once again cannot be excluded.

The uncertainty in the absolute energies of the various spectral features in Fig. 8 is estimated to be ± 3 eV. The energies of these features relative to the assumed series limit are more accurately measurable because of the rather well-defined falloff in intensity in the spectrum at this energy value. The peak at 101 ± 3 eV agrees well with a recent unpublished calculation of Weiss[28] of the energies of the ^4S, ^4P, and ^4D states whose dominant configurations are all $2p^5 3s 3p$. Weiss[28] also estimates that the energy of the $(2s2p^6 3s3p)\ ^4P$ state in Cl^{6+} is approximately 170 eV, which is close to a less prominent spectral feature in Fig. 8. Estimates of the energies of core-excited configurations such as $2p^5 3sns$ $(n \geq 4)$, $2p^5 3snp$ $(n \geq 3)$, and $2p^5 3p^2$ can be made using simple screening rules, and while the accuracy of this method is not sufficient to positively identify the observed lines, the results do show that several of the spectral features could be accounted for by the aforementioned configurations of eleven-electron chlorine ions.

The decay characteristics of the most prominent peaks in Fig. 8 were studied by changing the foil-target distance relative to the spectrometer viewing region over a range of approximately 25 cm. The indication is that the metastable autoionizing states associated with the prominent spectral peaks are very long lived. A more detailed study was made of the decay in flight of the 182 ± 3 eV peak by the standard method of measuring the count rate (per unit beam current) as a function of target position. The resulting decay curve was found to be complex in the sense that more than one exponential was needed to fit the data. It was obvious, however, that the decay curve had a very long-lived component associated with it, the decay rate of which was difficult to measure accurately because of the scatter in data points at large distances from the foil. We can thus quote only a lower limit of 43 nsec on the lifetime of a long-lived component associated with the 182 ± 3 eV peak. To explain the high metastability of these states, one may postulate the population of a level of high total spin and maximum total angular momentum which cannot directly autoionize via the Coulomb interaction or mix with close-lying fast-decaying autoionizing states of a different multiplicity. Such a level would presumably autoionize via the weaker spin-spin interaction. The level must also be metastable against radiative decay, which one would expect of a level of high spin and total angular momentum.

Lifetimes

In this section we summarize lifetime information that has previously been published[2] for the purpose of completeness. The lifetimes of the $J = \frac{5}{2}$ levels of the $(1s2s2p)\ ^4P^o$ (1) state of three-electron oxygen, fluorine, chlorine, and argon are shown in Table III along with some theoretical estimates of these lifetimes made by Manson[18] and Balashov *et al.*[19] Agreement is marginal between our result for O^{5+} and the results of Dmitriev *et al.*[17] The results were obtained by observing the decay in flight of the autoionization electrons from the $(1s2s2p)\ ^4P^o_{5/2}$ level as the foil target was translated parallel to the beam axis, thus changing the relative distance between the foil and the spectrometer viewing region. There exists a differential metastability within the fine-structure levels of the $(1s2s2p)\ ^4P^o$ state due to the different strengths of their coupling to the adjacent doublet continuum. The $J = \frac{1}{2}$ and $\frac{3}{2}$ levels can couple to the doublet continuum states via the spin-orbit, spin-other-orbit, and spin-spin interactions. They are also able to mix to some extent with the $J = \frac{1}{2}$ and $\frac{3}{2}$ levels of the $(1s2s2p)\ ^2P^o$ state, which themselves can make allowed autoionization transitions to doublet continuum states. The $J = \frac{5}{2}$ level, however, can only autoionize through the tensor part of the spin-spin interaction and is thus expected to be more metastable than the $J = \frac{1}{2}$ and $\frac{3}{2}$ components. The differential metastability between the $J = \frac{1}{2}, \frac{3}{2}$, and $\frac{5}{2}$ levels was used to our advantage in the measurements of the lifetimes of the $(1s2s2p)\ ^4P^o_{5/2}$ levels since the decay measurements were begun far enough downstream from the foil that the shorter lived $J = \frac{1}{2}$ and $\frac{3}{2}$ components had effectively decayed away. The decay curve in this situation was a single exponential, from which the $J = \frac{5}{2}$ level lifetime could be extracted by a simple least-squares fit. Figure 9 shows a plot of the decay probability γ of the $(1s2s2p)\ ^4P^o_{5/2}$ level of three-electron ions against a screened Z, on the assumption that the spin-spin autoionization process is the only decay channel that depopulates the state. The plotted points in this figure are all derived from both experi-

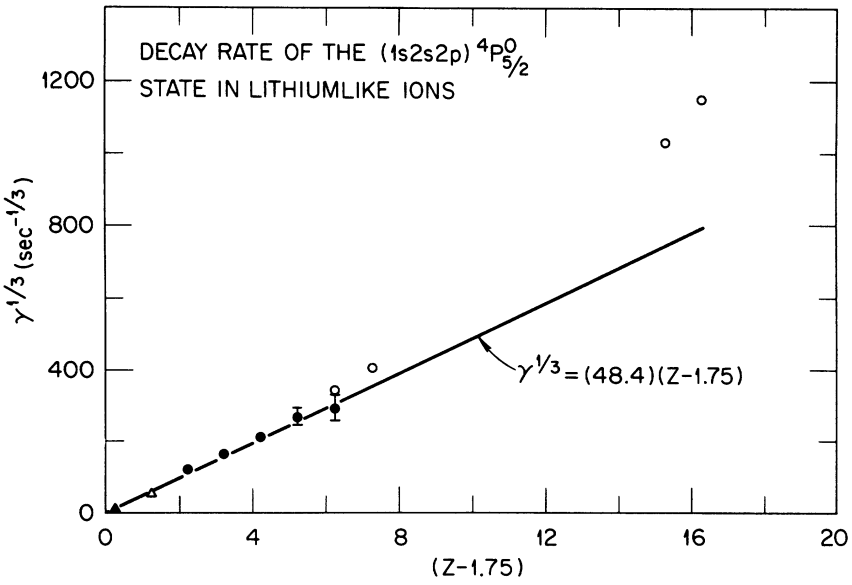

FIG. 9. Decay rate (inverse lifetime) of the $(1s2s2p)\,^4P^0_{5/2}$ level in some three-electron ions, assuming no radiative branching. The figure shows experimental decay rates taken to the one-third power plotted against an effective charge, $Z-1.75$. ▲(Ref. 16); △(Ref. 15); ● (Ref. 17); ○ (present work).

mental and theoretical investigations, including our results. A semiempirical scaling rule that was suggested by Levitt, Novick, and Feldman[29] for three-electron ions of low Z is also drawn (solid curve) in Fig. 9. While this fit appears quite good for the low-Z systems, our results show that there begins to be a serious departure from the empirical fit in the case of high-Z ions. It is clear that better theoretical lifetime values are needed for high-Z systems where higher-order relativistic effects may be important. Part, but not all, of the observed departure can be explained by assuming that a forbidden radiative channel of decay also begins to open up for these high-Z ions and thus compete with spin-spin induced autoionization for depopulation of the $(1s2s2p)\,^4P^o_{5/2}$ level. An $M2$ radiative transition $[(1s^22s)\,^2S^e_{1/2}-(1s2s2p)\,^4P^o_{5/2}]$ to the ground state of the three-electron ion has been recently observed by Cocke *et al.*,[20] in three-electron chlorine ions.

The decays in flight of several other features of the oxygen and fluorine spectra were studied. The second, third (peak A), and fourth (peak B) peaks were found to have complex decay curves, in the sense that more than one exponential was clearly needed to fit the data. (In each case fast components of order 1 nsec or less were present.) Only the decay curve for the most intense features of the oxygen spectrum shown in Fig. 7 was found to be a single exponential over an appreciable interval (~3 decay lengths) yielding a lifetime of $(1.00\pm0.04)\times10^{-9}$ sec. This indicates that only one state of the several encompassed by this feature (see Table I) was dominant in decay over this time range.

The occurrence of highly excited metastable autoionizing states of high spins and angular momenta seems to be quite a general phenomenon. We have described the observations of forbidden autoionizing decays of such states in at least three-, four-, five-, and eleven-electron systems using a foil-excitation method. Whether these states will be observable in autoionizing decay by a method such as that described here, will depend primarily upon the electron-energy range observed and the lifetimes of the states. Autoionization electrons of low energy are more difficult to study experimentally by this method owing to both the increased effects of stray magnetic fields and the considerable amount of low-energy knock-on electron background coming from the foil target. The lifetime of a state is, in general, determined by the combined probabilities for both autoionizing and radiative decay processes. If the branching ratio for radiative decay is large in comparison with that for autoionization, the autoionizing process will, of course, be difficult to observe. Nonetheless, it appears there may be a great many such states (associated with a wide variety of ions) awaiting discovery whose energies and lifetimes can be studied by the methods outlined here and by improvements thereof.

The yield per incident ion of the $(1s2s2p)\,^4P^o_{5/2}$ state was measured in oxygen and fluorine in order to determine how commonly these states are formed in a foil-excited beam. The results indicated that for this single state alone, the peak yield was of the order of 1% per incident ion. It

then seems probable that > 1% of the excited beam is metastable to some degree when other states and ions are considered.

The dearth of calculations of the lifetimes of metastable autoionizing states is particularly apparent and identifications would be greatly aided by such information.

ACKNOWLEDGMENTS

The research described here required extensive support from a large number of staff members of the Oak Ridge National Laboratory. We would like to acknowledge the contributions of the ORNL tandem and cyclotron staffs, particularly those of F. DiCarlo, D. Galbraith, P. Griffin, D. Hensley, J.W. Johnson, M. Loftus, B. Luttrell, C. Moak, A. Rikkola, P. Stelson, R. Ward, and G. Wells. We acknowledge also the continuing interest, advice, and contributions of Professor Bailey Donnally, who played a principal role in developing the first experiments of this type (see Ref. 2).

---

*Research sponsored in part by the University of Tennessee under contract with the Office of Naval Research and by Union Carbide Corporation, Kansas State University, and Oak Ridge Associated Universities under contracts with the Atomic Energy Commission.

[1]B. R. Junker and J. N. Bardsley, preceding paper, Phys. Rev. A **8**, 1345 (1973).

[2]B. Donnally, W. W. Smith, D. J. Pegg, M. Brown, and I. A. Sellin, Phys. Rev. A **4**, 122 (1971); I. A. Sellin, D. J. Pegg, M. Brown, W. W. Smith, and B. Donnally, Phys. Rev. Lett. **27**, 1108 (1971); I. A. Sellin, D. J. Pegg, P. M. Griffin, and W. W. Smith, Phys. Rev. Lett. **28**, 1229 (1972); D. J. Pegg, I. A. Sellin, P. M. Griffin, and W. W. Smith, Phys. Rev. Lett. **28**, 1615 (1972); W. W. Smith, B. Donnally, D. J. Pegg, P. M. Griffin, and I. A. Sellin, Phys. Rev. A **7**, 487 (1973).

[3]J. W. Hiby, Ann. Phys. (Leipz.) **34**, 473 (1939); R. Dopel, Ann. Phys. (N.Y.) **76**, 1 (1925).

[4]T-Y. Wu, Phys. Rev. **58**, 1114 (1940).

[5]T-Y. Wu and S. T. Shen, Chin. J. Phys. (Peking) 5, 150(1944).

[6]E. Holøien and J. Midtal, Proc. Phys. Soc. Lond. A **68**, 815 (1955).

[7]J. D. Garcia and J. E. Mack, Phys. Rev. **138**, A987 (1965).

[8]E. Holøien and S. Geltman, Phys. Rev. **153**, 81 (1967).

[9]G. Herzberg and H. R. Moore, Can. J. Phys. **37**, 1239 (1959).

[10]H. Schuler, Ann. Phys. (Leipz.) **76**, 292 (1925); S. Werner, Nature (Lond.) **118**, 154 (1926).

[11]J. P. Buchet, A. Denis, J. Desesquelles, and M. Dufay, Phys. Lett. A **28**, 529 (1969); W. S. Bickel, I. Bergstrom, R. Buchta, L. Lundin, and I. Martinson, Phys. Rev. **178**, 118 (1969); W. S. Bickel, I. Martinson, L. Lundin, R. Buchta, J. Bromander, and I. Bergstrom, J. Opt. Soc. Am. **59**, 830 (1969); F. Gaillard, M. Gaillard, J. Desesquelles, and M. Dufay, C.R. Acad. Sci. (Paris) **269**, 420 (1969); N. Anderson, R. Boleau, K. Jenson, and E. Veje, Phys. Lett. A **34**, 227 (1971); H. G. Berry, J. Bromander, I. Martinson, and R. Buchta, Phys. Scr. **3**, 63 (1971); H. G. Berry, E. H. Pinnington, and J. L. Subtil, J. Opt. Soc. Am. **62**, 767 (1972); S. Hontzeas, I. Martinson, P. Erman, and R. Buchta, Phys. Scr. **6**, 55 (1972).

[12]B. Edlén and F. Tyrén, Nature (Lond.) **143**, 940 (1939).

[13]N. J. Peacock, R. J. Speer, and M. G. Hobby, J. Phys. B **2**, 798 (1969); A. H. Gabriel and C. Jordan, Nature (Lond.) **221**, 947 (1969).

[14]A. B. C. Walker, Jr. and H. R. Rugge, Astrophys. J. **164**, 181 (1971); G. A. Doscheck, J. F. Meekins, R. W. Kreplin, T. A. Chubb, and H. Friedman, Astrophys. J. **164**, 165 (1971).

[15]P. Feldman and R. Novick, Phys. Rev. Lett. **11**, 278 (1963); Phys. Rev. **160**, 143 (1967).

[16]L. M. Blau, R. Novick, and D. Weinflash, Phys. Rev. Lett. **24**, 1268 (1970).

[17]I. S. Dmitriev, V. S. Nikolaev, and Ya. A. Teplova, Phys. Lett. A **26**, 122 (1968); I. S. Dmitriev, L. I. Vinogradova, V. S. Nikolaev, and B. M. Pepov, Zh. Eksp. Teor. Fiz. Pis'ma Red. **3**, 35 (1966) [JETP Lett. **3**, 20 (1966)].

[18]S. T. Manson, Phys. Lett. **23**, 315 (1966).

[19]V. V. Balashov, V. S. Senashenko, and B. Tekou, Phys. Lett. A **25**, 487 (1967).

[20]L. Cocke, B. Curnutte, and J. MacDonald, in Proceedings of the Third International Conference on Beam-Foil Spectroscopy Nucl. Instr. Methods (to be published).

[21]V. V. Zashkvara, M. I. Korsuskii, and O. S. Kosmachev, Zh. Tekh. Fiz. **36**, 132 (1966) [Sov. Phys.-Tech. Phys. **11**, 96 (1966)].

[22]H. G. Berry, Phys. Rev. A **6**, 514 (1972).

[23]E. Holøien and J. Midtal, J. Phys. B **4**, 1243 (1971).

[24]I. A. Sellin, D. J. Pegg, M. Brown, W. W. Smith, and B. Donnally, Phys. Rev. Lett. **27**, 1108 (1971).

[25]C. E. Moore, *Ionization Potentials and Ionization Limits Derived from the Analysis of Optical Spectra*, Natl. Bur. Std. Ref. Data Series No. NSRDS-NBS34 (U.S. GPO, Washington, D. C., 1970).

[26]I. A. Sellin, D. J. Pegg, P. M. Griffin, and W. W. Smith, Phys. Rev. Lett. **28**, 1229 (1972).

[27]R. Snyder (private communication).

[28]A. Weiss (private communication).

[29]M. Levitt, R. Novick, and P. Feldman, Phys. Rev. A **3**, 130 (1971).